

A histone fold TAF octamer within the yeast TFIID transcriptional coactivator

William Selleck¹, Ryan Howley¹, Qiaojun Fang^{1,2}, Vladimir Podolny³, Michael G. Fried⁴, Stephen Buratowski³ and Song Tan¹

¹Center for Gene Regulation, Department of Biochemistry & Molecular Biology, The Pennsylvania State University, University Park, Pennsylvania 16802-1014, USA. ²Present address: Department of Biological Chemistry, Johns Hopkins School of Medicine, Baltimore, Maryland 21205, USA. ³Department of Biological Chemistry and Molecular Pharmacology, Harvard Medical School, Boston, Massachusetts 02115, USA. ⁴Department of Biochemistry and Molecular Biology, The Pennsylvania State University College of Medicine, Hershey, Pennsylvania 17033, USA.

Gene activity in a eukaryotic cell is regulated by accessory factors to RNA polymerase II, which include the general transcription factor complex TFIID, composed of TBP and TBP-associated factors (TAFs). Three TAFs that contain histone fold motifs (yTAF17, yTAF60 and yTAF61) are critical for transcriptional regulation in the yeast *Saccharomyces cerevisiae* and are found in both TFIID and SAGA, a multicomponent histone acetyltransferase transcriptional coactivator. Although these three TAFs were proposed to assemble into a pseudooctamer complex, we find instead that yTAF17, yTAF60 and yTAF61 form a specific TAF octamer complex with a fourth TAF found in TFIID, yTAF48. We have reconstituted this complex *in vitro* and established that it is an octamer containing two copies each of the four components. Point mutations within the histone folds disrupt the octamer *in vitro*, and temperature-sensitive mutations in the histone folds can be specifically suppressed by overexpressing the other TAF octamer components *in vivo*. Our results indicate that the TAF octamer is similar both in stoichiometry and histone fold interactions to the histone octamer component of chromatin.

Both the general transcription factor complex, TFIID, and a multicomponent histone acetyltransferase transcriptional coactivator, SAGA, contain proteins that have the same histone fold found in chromatin^{1–3}. The histone fold is a helix-loop-helix-loop-helix motif common to the core histones H2A, H2B, H3 and H4 (Fig. 1a), which make up the histone octamer. Crystallographic studies of the histone octamer⁴ and the nucleosome core particle⁵ show that the histone octamer contains one H3₂H4₂ heterotetramer flanked on either side by an H2A–H2B heterodimer, with intimate histone fold interactions responsible for each of the interhistone contacts (Fig. 1b). Because of the structural similarity of the *Drosophila* homolog of the yTAF17–yTAF60 complex to the H3₂H4₂ tetramer⁶, pairwise interaction studies and the apparent absence of an H2A-like TAF, the three histone fold TAFs (TAF17, TAF60 and TAF61 in yeast) were proposed to form an octameric structure. This model contains two H2B-like homodimers (yTAF61)₂ bound to a H3₂H4₂-like heterotetramer⁷ (yTAF17–yTAF60)₂; however, this pseudo histone fold TAF octamer has not been detected experimentally. Furthermore, more recent studies predict that other TFIID components, including yTAF19, yTAF25, yTAF40, yTAF47, yTAF48 and yTAF65, also contain the histone fold motif^{8–11}. Thus, TFIID contains at least nine TAF proteins with the histone fold motif, and whether these can assemble into an octamer substructure is not known. Because the composition and structure of the histone fold complexes will provide valuable insight into the internal arrangement and function of these coactivators, determination of which, if any, of the histone fold subunits form a histone octamer-like complex is important. In this work, we show that yTAF17, yTAF60, yTAF61 and yTAF48 form a TAF octamer complex with significant similarities to the histone octamer.

yTAF17–yTAF60–yTAF61c–yTAF48 form a complex

Recent findings have shown that human TAF20 and TAF130 polypeptides form a H2A–H2B-like heterodimer¹² and that yeast TFIID contains a previously unaccounted for hTAF130/dTAF110 homolog, yTAF48 (also known as Mpt1 and Tsg2)^{10,11}. Sequence, structural and biochemical analyses^{2,3,12} suggest that yTAF17, yTAF60, yTAF61 and yTAF48 are

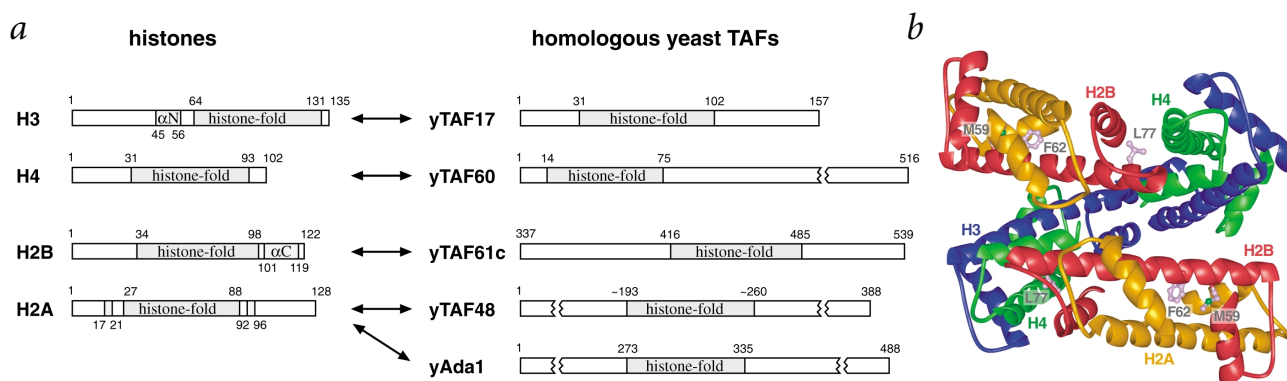


Fig. 1 The histone fold motif in histones and histone fold TAFs. **a**, Schematic of histone fold motif in histone proteins and histone fold TAFs. Histones H3, H4, H2A and H2B each contain one histone fold motif. H3 and H2B contain additional N- and C-terminal α -helices, respectively, whereas H2A contains short α -helices on either side of the histone fold⁵. The yTAF17, yTAF60, yTAF48 and yTAF61 polypeptides used in this study are shown, as well as the yAda1 polypeptide. Each contains one histone fold motif as deduced from sequence similarity. The yTAF61c = yTAF61(337–539) truncation used includes the conserved region sufficient for viability of the yeast cell¹⁴. **b**, Ribbon representation of the structure of the core histones of the *Xenopus* histone octamer from the nucleosome core particle⁵. The H3 and H4 polypeptides are shown in blue and green, respectively, and H2A and H2B are shown in yellow and red, respectively. The side chains of three important residues involved in heterodimer and octamer formation are shown. H2B Met 59 and Phe 62 are at the hydrophobic four-helix bundle interface between H2A and H2B in the heterodimer. H2B Leu 77 is situated in the two hydrophobic four-helix bundle interfaces between H2B and H4, which hold the H2A–H2B heterodimers to the H3₂H4₂ heterotetramer to form the octamer.

letters

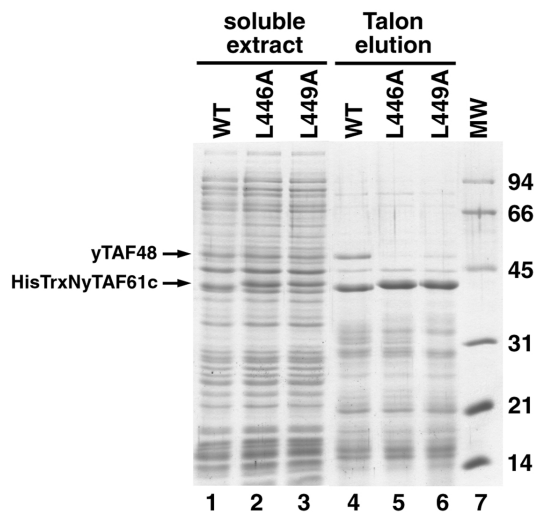


Fig. 2 Formation of the yTAF61c–yTAF48 complex requires the histone fold. Soluble extracts of cells coexpressing HisTrxNyTAF61c, HisTrxNyTAF61c(L446A) or HisTrxNyTAF61c(L449A) with yTAF48 (lanes 1–3) were incubated with Talon cobalt-based affinity resin. The resin was washed and eluted with 100 mM imidazole (lanes 4–6). Molecular weight markers are shown in lane 7. The slight mobility difference of the HisTrxNyTAF61c mutants compared with wild type protein is presumably due to the site directed mutations, because DNA sequencing did not detect any difference between the expression plasmids aside from the engineered mutations. The HisTrxN portion of the HisTrxNyTAF61c polypeptide stains particularly well with Coomassie Blue used in the gel shown (data not shown).

homologous in their histone fold regions to the H3, H4, H2B and H2A components of the histone octamer, respectively, prompting us to ask whether these four yeast TAF proteins could form a complex.

We have utilized a newly developed bacterial polycistronic expression vector¹³ to coexpress, reconstitute and purify yeast yTAF61c–yTAF48 and yTAF17–yTAF60 complexes. The yTAF61c construct lacks the first 336 amino acids of yTAF61, which are not required for viability of yeast cells¹⁴. Coexpressed, His-tagged yTAF61c and yTAF48 copurify over metal affinity, anion-exchange and size exclusion chromatography (Fig. 2, lanes 1 and 4; Fig. 3b; data not shown), whereas neither recombinant, His-tagged yTAF61c nor recombinant yTAF48 binds to the metal affinity column on its own (data not shown). This suggests that yTAF61(337–539) is sufficient for complex formation with yTAF48. Furthermore, the histone folds of yTAF61 and yTAF48 are required for their interactions because yTAF61 point mutations L446A or L449A in the putative yTAF48–yTAF61 histone fold interface (equivalent to *Xenopus laevis* H2B Met 59 and Phe 62 located in the histone H2A–H2B interface; Fig. 1b) disrupt formation of the yTAF61c–yTAF48 complex (Fig. 2, lanes 2, 3, 5 and 6). We also find that components of the His-tagged yTAF17–yTAF60 complex coexpressed in *Escherichia coli* copurify over metal-affinity, anion-exchange and size exclusion chromatography (Fig. 3d, data not shown), whereas yTAF17 expressed under the same conditions is insoluble (see Fig. 6 in ref. 13).

In contrast to the histone octamer, which is stable only in high salt conditions¹⁵, the yTAF17–yTAF60–yTAF61c–yTAF48 complex can be reconstituted simply by incubating purified, untagged yTAF17–yTAF60 and yTAF61c–yTAF48 complexes together in moderate salt conditions. Size exclusion chromatography of the reconstitution mix shows a new peak, as compared to the individual yTAF17–yTAF60 and yTAF61c–yTAF48 peaks, with estimated molecular weight of 293 ± 27 kDa for a globular complex, comparable to the expected molecular weight of 280 kDa for the TAF octamer (Fig. 3a,e). Analysis of the chromatographic fractions by SDS-PAGE show that all four polypeptides coelute in this peak (Fig. 3f, lane 2). Because this chromatographic profile is different from the yTAF17–yTAF60 and yTAF61c–yTAF48 complexes, which both elute later (Fig. 3a,b,d), yTAF17–yTAF60–yTAF61c–yTAF48 must form a new complex

Histone fold interactions in the TAF complex

In the histone octamer, two copies of the H2A–H2B dimer bind each side of the central H3₂H4₂ tetramer through H2B and H4 interactions that create four-helix bundles^{4,5} (Fig. 1b). To determine if the yTAF17–yTAF60–yTAF61–yTAF48 interactions are specific and to examine the role of the histone motif in the complex formation, we created single point mutants that potentially disrupt the H2B–H4-like interface in yTAF61–yTAF60. Both examination of the histone octamer in the nucleosome core particle structure and sequence alignments suggested Leu 464 in yTAF61 as a target for mutation, because the equivalent H2B residue, Leu 77 in *X. laevis*, is located in the hydrophobic core of the H2B–H4 four-helix bundle (Fig. 1b). Also, this Leu residue is highly conserved among both the histone and TAF families. As anticipated, yTAF61c(L464A) coexpresses and copurifies with yTAF48 comparable to the wild type polypeptide (Fig. 3b,c; data not shown), indicating that this mutation does not disrupt the yTAF61–yTAF48 interface. However, this mutant polypeptide does not reconstitute with yTAF17, yTAF60 and yTAF48 to form the yTAF17–yTAF60–yTAF61c–yTAF48 complex. Instead, reconstitution mixes of yTAF17–yTAF60 and yTAF61c(L464A)–yTAF48 elute from the size exclusion column as the superposition of the yTAF17–yTAF60 and yTAF61c–yTAF48 peaks (Fig. 3g). Thus, the histone fold is required for the formation of the yTAF17–yTAF60–yTAF61c–yTAF48 complex, and the interactions between yTAF17–yTAF60 and yTAF61c–yTAF48 are specific. Similar results were observed with a separate point mutation of yTAF61 in which the same Leu residue is replaced with a bulkier Tyr residue (yTAF61(L464Y)) (data not shown).

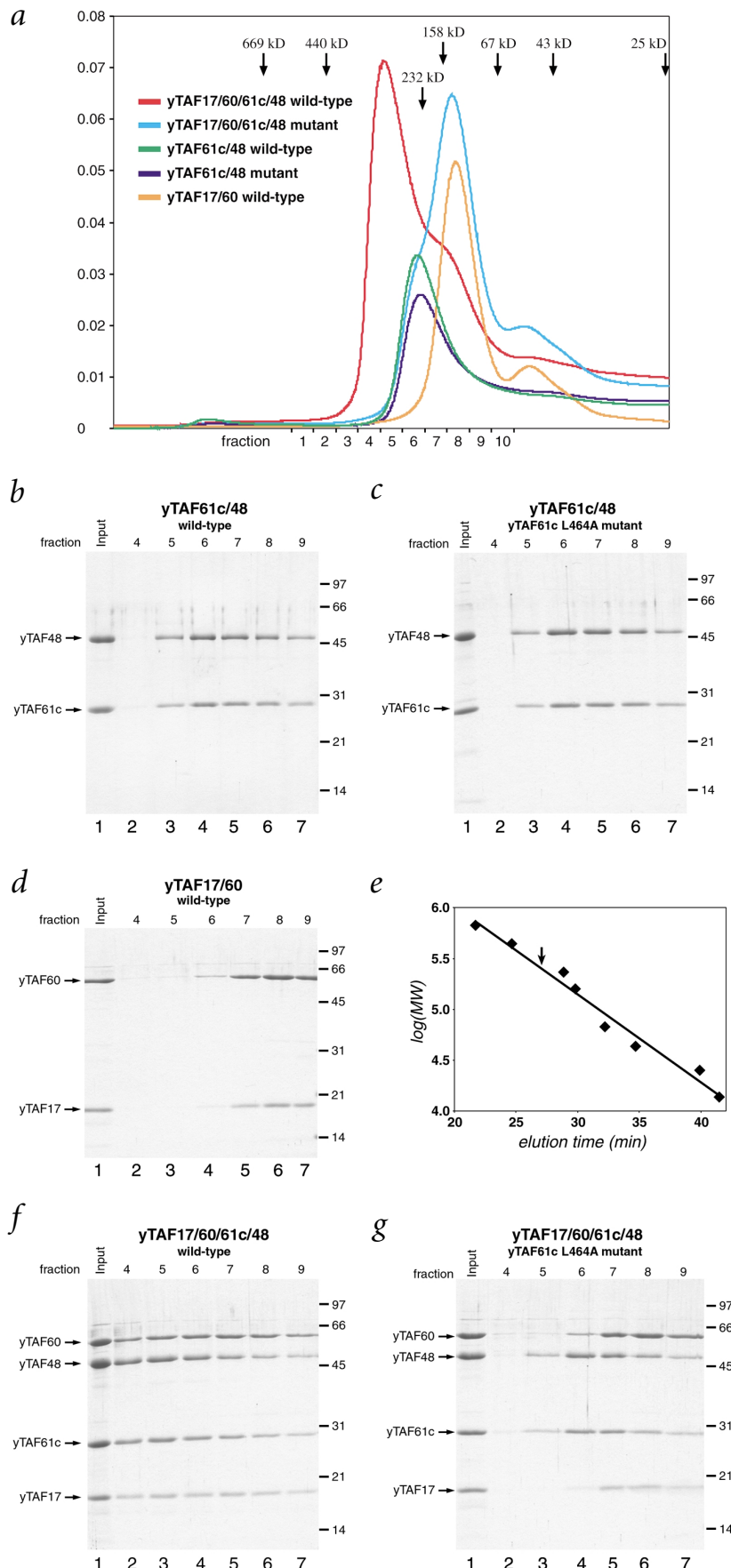
The yTAF17–yTAF60–yTAF61c–yTAF48 complex is an octamer

The yTAF17–yTAF60–yTAF61c–yTAF48 complex eluted from size exclusion chromatography with a molecular weight consistent with a TAF octamer that contains two copies of each of the four proteins. However, because molecular weight estimates by size exclusion chromatography depend on both the size and shape of the complex, we sought independent confirmation for the stoichiometry of the TAF histone fold complex.

First, we performed quantitative HPLC to determine the relative stoichiometry of the four TAF components. We used fractions four and five of size exclusion purified TAF octamer (similar to Fig. 2) to remove excess yTAF17–yTAF60 and most of any excess yTAF61c–yTAF48 complexes. We then separated the yTAF17, yTAF60, yTAF61c and yTAF48 components in the complex by reverse phase chromatography under conditions allowing for the quantitative recovery of each component (Fig. 4a). The amount of protein in each peak was determined by measuring the area under the peak and correcting for the calculated extinction coefficient of each protein. We find that



Fig. 3 Formation and specificity of the TAF histone fold complex. **a**, Size exclusion chromatography of yTAF17–yTAF60 (yellow), yTAF61c–yTAF48 (green) and reconstituted yTAF17–yTAF60–yTAF61c–yTAF48 (red) complexes, as well as the yTAF61c–yTAF48 mutant complex containing the yTAF61c(L464A) mutation (dark blue) and yTAF17–yTAF60–yTAF61c–yTAF48 mutant complex containing the yTAF61c(L464A) mutation (cyan) reconstitution mixes. Elution positions of molecular weight standards are shown above. Samples were chromatographed over Superdex 200 HR column, and 1 min fractions collected. **b–d**, SDS-PAGE of starting material (Input) and fractions 4–9 for the yTAF61c–yTAF48, yTAF61c(L464A)–yTAF48 and yTAF17–yTAF60 complexes, respectively. **e**, Calibration curve for molecular weight standards. The position of the yTAF17–yTAF60–yTAF61c–yTAF48 complex is shown by the arrow. **f,g**, SDS-PAGE of starting material (Input) and fractions 4–9 for yTAF17–yTAF60–yTAF61c–yTAF48 and yTAF17–yTAF60–yTAF61c(L464A)–yTAF48 reconstitution mixes, respectively.



yTAF17, yTAF60, yTAF61c and yTAF48 are present in the TAF complex with molar abundance of 1.00, 1.06 ± 0.04 , 1.34 ± 0.11 and 1.29 ± 0.19 , respectively, relative to yTAF17. These results are close to a 1:1:1:1 ratio for the four proteins. The slightly higher ratio of the yTAF61c–yTAF48 components may result from incomplete fractionation of the yTAF17–yTAF60–yTAF61c–yTAF48 complex from yTAF61c–yTAF48 by size exclusion chromatography.

Second, we performed sedimentation equilibrium ultracentrifugation to determine the molecular weight of the yTAF17–yTAF60–yTAF61c–yTAF48 complex. The data from a representative sedimentation profile of the TAF complex is described well by a single-species model, as demonstrated by the small, symmetrically distributed residuals (Fig. 4b). The molecular weight returned by this analysis was 285.1 ± 9.0 kDa, consistent with the expected molecular weight of 280.0 kDa for the TAF octamer. The inclusion of a second independent species in the sedimentation model did not improve the quality of the fit and yielded values of the second concentration term that were, within error, equal to zero (data not shown). Although this does not rule out the presence of additional species, such species are not present at significant levels in these samples.

Because the HPLC quantitation suggests that the TAF histone fold complex contains equimolar quantities of yTAF17, yTAF60, yTAF61c and yTAF48, and sedimentation equilibrium ultracentrifugation studies point to a single species with molecular weight of ~285 kDa, we conclude that the TAF complex of yTAF17–yTAF60–yTAF61c–yTAF48 is an octamer containing two copies each of the four proteins.

letters

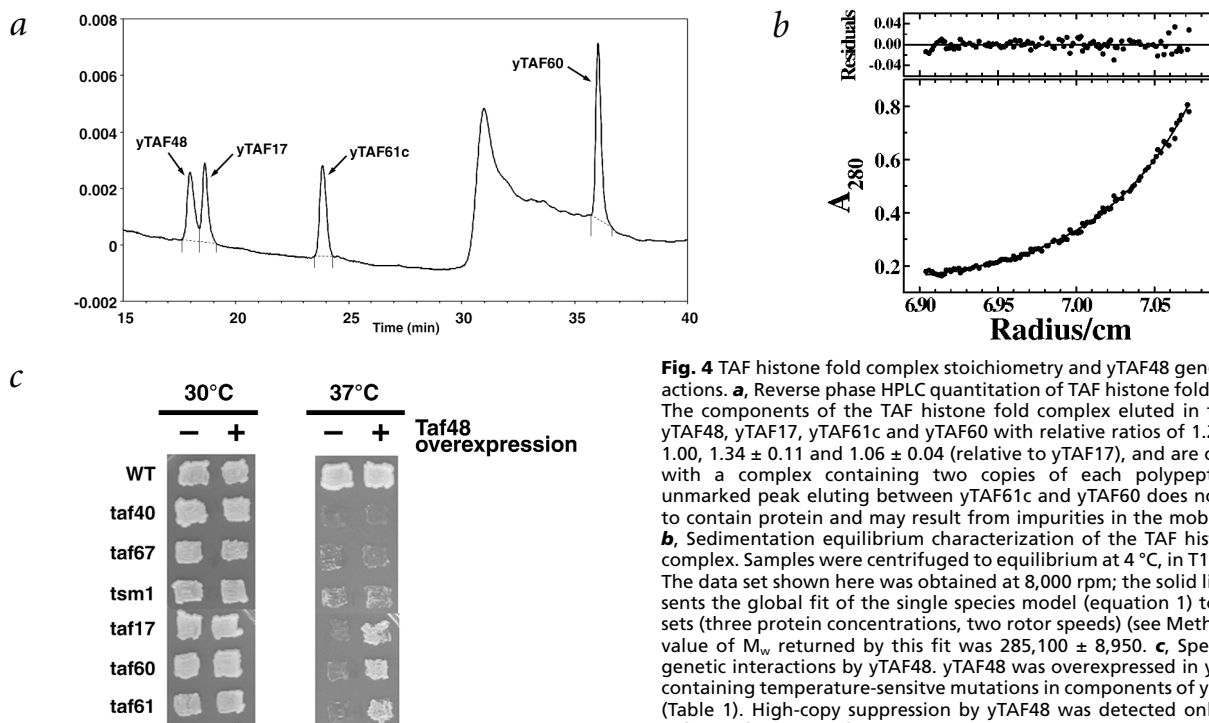


Fig. 4 TAF histone fold complex stoichiometry and yTAF48 genetic interactions. **a**, Reverse phase HPLC quantitation of TAF histone fold complex. The components of the TAF histone fold complex eluted in the order yTAF48, yTAF17, yTAF61c and yTAF60 with relative ratios of 1.29 ± 0.19 , 1.00 , 1.34 ± 0.11 and 1.06 ± 0.04 (relative to yTAF17), and are consistent with a complex containing two copies of each polypeptide. The unmarked peak eluting between yTAF61c and yTAF60 does not appear to contain protein and may result from impurities in the mobile phase. **b**, Sedimentation equilibrium characterization of the TAF histone fold complex. Samples were centrifuged to equilibrium at 4°C , in T100 buffer. The data set shown here was obtained at 8,000 rpm; the solid line represents the global fit of the single species model (equation 1) to six data sets (three protein concentrations, two rotor speeds) (see Methods). The value of M_w returned by this fit was $285,100 \pm 8,950$. **c**, Specificity of genetic interactions by yTAF48. yTAF48 was overexpressed in yeast cells containing temperature-sensitive mutations in components of yeast TFIID (Table 1). High-copy suppression by yTAF48 was detected only for the *taf17*, *taf60* and *taf61* alleles, which suggests that yTAF48 interacts specifically with yTAF17, yTAF60 and yTAF61 in the yeast cell.

Specificity and *in vivo* relevance

Our *in vitro* data that demonstrate the formation of a TAF histone fold octamer suggest that yTAF17, yTAF60, yTAF61 and yTAF48 form a TAF histone fold subcomplex in the yeast TFIID complex. Previous *in vivo* studies have shown that overexpression of yTAF60 or yTAF61 suppresses the temperature-sensitive *taf17(L68P)* mutant, whereas overexpression of other TAFs, including another histone fold TAF, yTAF40, did not¹⁶. Similarly, the *taf60(V41P)* mutation was suppressed by overexpression of yTAF17 or yTAF61 but not by yTAF40 and other TAFs¹⁶. In contrast, the *taf40-3100* allele was suppressed only by yTAF19 overexpression and not by yTAF17, yTAF60 or yTAF61¹⁷.

We now extend these results to include yTAF48. Overexpression of yTAF48 suppresses temperature-sensitive mutations in yTAF17, yTAF60 and yTAF61 but not in yTAF40, yTAF67 or TSM1 (Fig. 4c, Table 1). Furthermore, a temperature-sensitive allele of yTAF48 mutated in the histone fold region (N204D) is suppressed by overexpression of yTAF61 but not by yTAF17, yTAF60, yTAF19 or yTAF40 (Table 1; data not shown). These and the previous published suppression data demonstrate a genetic interaction between yTAF17, yTAF60, yTAF61 and yTAF48. Furthermore, the interaction is specific since overexpression of yTAF19 or yTAF40, which both contain histone fold motifs, does not suppress temperature-sensitive alleles of yTAF17, yTAF60, yTAF61 or yTAF48. Conversely, overexpression of yTAF17, yTAF60, yTAF61 or yTAF48 does not suppress a temperature-sensitive allele of yTAF40. This suggests that the presumed yTAF40–yTAF19 heterodimer homolog of hTAF28–hTAF18, whose histone fold structure was determined crystallographically⁹, does not make histone fold interactions with yTAF17, yTAF60, yTAF61 or yTAF48, and provides further evidence that yTAF17–yTAF60–yTAF61–yTAF48 is a native subcomplex of yeast TFIID.

Discussion

Our results suggest that TFIID contains a TAF octamer subcomplex that involves histone fold interactions between the component proteins. This subcomplex exhibits similarities to the histone octamer in both its stoichiometry and specific histone fold interactions. In particular, our size exclusion, quantitative HPLC and sedimentation equilibrium studies show that yTAF17, yTAF60, yTAF61 and yTAF48 form an octamer complex containing two copies each of these four polypeptides. The complex involves specific interactions between the histone folds because point mutations in the histone fold disrupt the complex *in vitro* and mutations in the histone folds can be suppressed only when the appropriate partners are overexpressed *in vivo*. Furthermore, we find that neither yTAF17–yTAF60 nor yTAF61c–yTAF48 forms a stable complex with the yTAF40–yTAF19 histone fold pair that is also found in TFIID, with the possible exception of weak interactions that do not appear to involve histone fold contacts (unpublished data).

We believe for several reasons that the TAF octamer of yTAF17–yTAF60–yTAF61–yTAF48 contains a central yTAF17₂–yTAF60₂ tetramer flanked on either side by yTAF61–yTAF48. First, sequence analysis suggests that yTAF17, yTAF60, yTAF61 and yTAF48 are homologous in their histone folds to H3, H4, H2B and H2A, respectively. Second, the *Drosophila* homolog of the yTAF17–yTAF60 complex histone fold core (dTAF42–dTAF62) bears strong structural similarities to the histone H3₂H4₂ tetramer⁶. Thirdly, the yTAF61(L464A), yTAF61(L464Y), yTAF61(L446A) and yTAF61(L449A) point mutants suggest that yTAF61 interacts with yTAF48 and yTAF60 in a similar manner to H2B interactions with H2A and H4 in the histone octamer. However, the possibility that yTAF17, yTAF60, yTAF61 and yTAF48 form an octamer with a different quaternary arrangement from the histone octamer cannot be excluded.

**Table 1 Genetic interaction of histone fold TAFs¹**

Gene	Temperature-sensitive mutants ²				
	<i>taf17</i>	<i>taf60</i>	<i>taf68</i>	<i>taf48</i>	<i>taf40</i>
overexpressed					
yTAF17	C ³	+ ³	- ³	-	- ⁴
yTAF60	+ ³	C ³	- ³	-	- ⁴
yTAF68	+ ³	+ ³	C	+	- ⁴
yTAF48	+	+	+	C	-
yTAF40	-	-	-	-	C ⁴
yTAF19	- ³	- ³	- ³	-	+ ⁴

¹+ = suppression of temperature-sensitive phenotype; - = no suppression of temperature-sensitive phenotype; and C = complementation of temperature-sensitive phenotype by wild type copy.

²*taf17* = taf17(L68P); *taf60* = taf60(V41P); *taf61* = taf61-23 = taf61(1-485), also true for taf61-12 = taf61(1-483) + Ile-Cys-Leu-Glu-Tyr; *taf48* = taf48(N204D); and *taf40* = taf40-3100 = Taf40(L147Q, C200W, L264S, T336A).

³Ref. 16.

⁴Ref. 17.

yTAF17, yTAF60, yTAF61c and yTAF48 form a stable octamer complex with a 2:2:2:2 stoichiometry that is not dependent on the stoichiometry of the yTAF17-yTAF60 or yTAF61c-yTAF48 complexes on their own. Although we have characterized the yTAF17-yTAF60 and yTAF61c-yTAF48 complexes by size-exclusion chromatography, we are unable to assign the stoichiometry within these complexes from this experiment because the size-exclusion elution profile is influenced by both size and shape of the complexes, and we cannot assume either complex is globular in shape. In addition, histone fold proteins associating with different stoichiometries on their own compared to the histone octamer has precedence. The histone proteins themselves can form complexes in addition to the canonical H2A-H2B heterodimer and H3₂H4₂ heterotetramer, depending on isolation or solution conditions¹⁵.

The SAGA complex contains yTAF17, yTAF60 and yTAF61 but does not appear to contain yTAF48 (refs 10,11,18), excluding the presence of the yTAF17-yTAF60-yTAF61-yTAF48 octamer in the SAGA complex. However, because SAGA contains yAda1, which has been shown to form a heterodimer with yTAF61 (ref. 12), it might contain an equivalent yTAF17-yTAF60-yTAF61-yAda1 histone fold complex, in which the SAGA-specific yAda1 replaces the TFIID-specific yTAF48 component. We have, in fact, reconstituted a yTAF17-yTAF60-yTAF61-yAda1 complex *in vitro* (unpublished data). Thus, TFIID and SAGA coactivators, which may function on a chromatin template, both contain histone fold subcomplexes that have similarities to the histone octamer component of chromatin.

What is the significance of the TAF histone fold octamer? One possibility is that the TAF octamer may bind DNA in a manner analogous to the histone octamer in the nucleosome core particle. The extended footprint of TFIID on promoter DNA¹⁹ and the identification of dTAF42 and dTAF62 (homologous to yTAF17 and yTAF60, respectively) as components of TFIID that can crosslink to a downstream promoter element²⁰ lend support to this hypothesis. However, many protein-DNA interactions in the nucleosome are made by basic histone residues interacting with the DNA phosphate backbone, and several of such basic histone residues are replaced by acidic residues in the homologous TAF proteins²¹. Our own preliminary experiments fail to detect interaction of the yTAF17-yTAF60-yTAF61c-yTAF48 complex with DNA (unpublished data). A second possibility for the significance of the TAF histone fold octamer is that the

H2A-H2B-like heterodimer component of the TAF and histone octamer might exchange during different steps of transcription initiation²².

A third possibility is that the histone fold octamer might constitute a convenient structural arrangement within the TFIID complex¹⁰⁻¹². The histone fold TAFs yTAF17, yTAF60, yTAF61 and yTAF48 are all significantly larger than the histone fold region presumed to be required for the integrity of the TAF octamer. These additional sequences may be important for other aspects of TFIID function. For example, the human and *Drosophila* homologs of yTAF17, hTAF32 and dTAF40 have been suggested to interact directly with activator proteins; however, this was demonstrated for hTAF32 and dTAF40 on their own and not in the context of the TFIID complex²³⁻²⁶. The ability to reconstitute the TAF histone fold octamer in relatively pure form will now allow directed investigations into its structural and functional significance.

Methods

Coexpression, purification and reconstitution of recombinant proteins. The genes for yTAF17, yTAF60, yTAF61 and yTAF48 were amplified from yeast genomic DNA, cloned into cloning vectors and sequenced across the entire coding regions. Standard procedures were used to subclone appropriate combinations into the T7 promoter-based polycistronic expression vector pST39-HisTrxN, which provides a combination His₆-thioredoxin-Nla recognition site-fusion tag at the 5' end of the first cistron¹³.

HisTrxNyTAF17-yTAF60 and HisTrxNyTAF61c-yTAF48 complexes were overexpressed in BL21(DE3)pLysS cells containing the appropriate polycistronic expression plasmids. Affinity purification over Talon cobalt-based affinity resin (Clontech) was performed in 50 mM sodium phosphate, pH 7.0, 100 mM NaCl, 1 mM benzamide and 5 mM 2-mercaptoethanol (P100 buffer), with 100 mM imidazole added to elute. The HisTrxN-fusion tag on the appropriate polypeptide was removed using the site-specific tobacco etch virus Nla protease²⁷, leaving behind a nonnative Gly-Ser at the N-terminus of the cleaved polypeptide. The yTAF17-yTAF60 complex was then purified to near homogeneity over SourceQ anion-exchange resin (Pharmacia), whereas the yTAF61c-yTAF48 complex was purified over SourceS cation-exchange resin (Pharmacia). Complexes were quantitated by UV absorption using calculated extinction coefficients²⁸ of 19,090, 37,610, 16,530 and 13,400 M⁻¹ cm⁻¹ and molecular weights of 17,327, 57,901, 22,476 and 42,336 g mol⁻¹ for yTAF17, yTAF60, yTAF61c and yTAF48, respectively.

The TAF histone fold complex was reconstituted by mixing yTAF17-yTAF60 with yTAF61c-yTAF48 in a 1:1 molar ratio, assuming that both yTAF17-yTAF60 and yTAF61c-yTAF48 exist as heterotetramers. The volumes used are unaffected if yTAF61c-yTAF48 exists in solution as a heterodimer. The reconstitution mixture of ~20 μM complex in T100 buffer (20 mM Tris-Cl, pH 8.0, 100 mM NaCl, 0.1 mM EDTA and 10 mM 2-mercaptoethanol) was incubated on ice for 10-16 h and fractionated over a Superdex 200 HR column (10 mm internal diameter × 300 mm length) in the same buffer at 0.4 ml min⁻¹. Molecular weight standards used were thyroglobulin (660 kDa), ferritin (440 kDa), catalase (232 kDa), aldolase (158 kDa), BSA (67 kDa), ovalbumin (43 kDa), chymotrypsinogen A (25 kDa) and ribonuclease (13.7 kDa).

HPLC quantitation. Fractions 4 and 5 of Superdex 200 HR purified TAF octamer complex were fractionated over a BioBasic Cyano reverse phase column (Keystone Scientific) in 0.1% TFA using an acetonitrile gradient. In control experiments, the same amount of TAF polypeptides present were detected on SDS-PAGE before and after reverse phase HPLC, which suggests essentially quantitative recovery of the polypeptides. The individual peaks from the reverse phase HPLC were integrated using BioCad SPRINT v.3 data analysis software.

Sedimentation equilibrium ultracentrifugation. Samples of the TAF octamer complex equilibrated with T100 buffer were



letters

brought to sedimentation equilibrium in a Beckman XL-A analytical ultracentrifuge fitted with an AN-60Ti rotor, operating at 4.0 ± 0.1 °C. Data sets were collected at two rotor speeds (6,000 rpm and 8,000 rpm) and three nominal protein concentrations (0.8, 0.4 and 0.2 mg ml⁻¹). Absorbance values were measured at 280 nm as functions of radial position. Five scans were averaged for each sample at each rotor speed. Approach to equilibrium was considered to be complete when replicate scans separated by ≥ 6 h were indistinguishable.

Absorbance versus radial position data were fit using equation 2 of McRorie and Voelker²⁹, which describes the distribution of a single ideal species at equilibrium. To use this equation the partial specific volume of the protein and the solvent density must be known. Partial specific volume was calculated from the amino acid composition of the TAF octamer by the method of Cohn and Edsall³⁰ and corrected for temperature according to McRorie and Voelker²⁹. The solvent density was measured using a Mettler density meter. Global analysis of multiple data sets was performed with the program NONLIN (<http://www.bbri.org/RASMB/rasmb.html>).

Isolation and use of temperature-sensitive alleles. The yTAF48 gene was amplified from yeast genomic DNA using PCR and subcloned into the yeast vectors pRS316, pRS315 and pRS426. A deletion of yTAF48 was constructed by cloning 3' and 5' flanking regions of yTAF48 into the polylinker of pRS303 to create pRS303-*taf48Δ::HIS3*. The construct was linearized and transformed into YSB455 to create YSB755 (*MATa/MATα; ura3-52/ura3-52; leu2Δ1/leu2Δ1; trp1Δ63/trp1Δ63; his3Δ200/his3Δ200; lys2Δ202/lys2Δ202; TAF48/taf48Δ::HIS3*). The resulting strain was transformed with pRS316-TAF48 and sporulated to create the plasmid shuffling strain YSB757 (*MATa; ura3-52; leu2Δ1; trp1Δ63; his3Δ200; lys2Δ202; taf48Δ::HIS3; (pRS316-TAF48)*). A temperature-sensitive allele of yTAF48 was isolated by plasmid shuffling to screen hydroxylamine-mutagenized clones of pRS315-TAF48.

Temperature-sensitive alleles of yTAF17, yTAF60, yTAF61 and yTAF40 have been described^{16,17}. Suppression was assayed by transforming the temperature-sensitive yeast strains with 2μ plasmids carrying the indicated TAF genes. After selection at the permissive temperature (30 °C), transformants were restreaked on selective plates at the nonpermissive temperature (37 °C) and checked for growth over five days.

Acknowledgments

We thank B. Schlansky and M. Song for technical assistance; C. Brown, J. Reese, B. Simpson and J. Workman for critical reading of the manuscript, and to the gene regulation community at Penn State for stimulating discussions. We are also grateful to T. Richmond, in whose laboratory preliminary studies for this project were initiated. This work was supported by NIH grants to M.F., S.B. and S.T. S.B. is a Leukemia and Lymphoma Society Scholar.

Correspondence should be addressed to S.T. email: sxt30@psu.edu

Received 19 January, 2001; accepted 13 April, 2001.

1. Sterner, D.E. & Berger, S.L. *Microbiol. Mol. Biol. Rev.* **64**, 435–459 (2000).
2. Hampsey, M. *Microbiol. Mol. Biol. Rev.* **62**, 465–503 (1998).
3. Albright, S.R. & Tjian, R. *Gene* **242**, 1–13 (2000).
4. Arents, G., Burlingame, R.W., Wang, B.C., Love, W.E. & Moudrianakis, E.N. *Proc. Natl. Acad. Sci. USA* **88**, 10148–10152 (1991).
5. Luger, K., Mader, A.W., Richmond, R.K., Sargent, D.F. & Richmond, T.J. *Nature* **389**, 251–260 (1997).
6. Xie, X. et al. *Nature* **380**, 316–322 (1996).
7. Hoffmann, A. et al. *Nature* **380**, 356–359 (1996).
8. Gangloff, Y.G. et al. *Mol. Cell. Biol.* **21**, 1841–1853 (2001).
9. Birck, C. et al. *Cell* **94**, 239–249 (1998).
10. Sanders, S.L. & Weil, P.A. *J. Biol. Chem.* **275**, 13895–13900 (2000).
11. Reese, J.C., Zhang, Z. & Kurpad, H. *J. Biol. Chem.* **275**, 17391–17398 (2000).
12. Gangloff, Y.G. et al. *Mol. Cell. Biol.* **20**, 340–351 (2000).
13. Tan, S. *Protein Expr. Purif.* **21**, 224–234. (2001).
14. Moqtaderi, Z., Yale, J.D., Struhl, K. & Buratowski, S. *Proc. Natl. Acad. Sci. USA* **93**, 14654–14658 (1996).
15. van Holde, K.E. In *Chromatin* (ed. Rich, A.) 162–168 (Springer-Verlag, New York; 1989).
16. Michel, B., Komarnitsky, P. & Buratowski, S. *Mol. Cell* **2**, 663–673 (1998).
17. Komarnitsky, P.B., Michel, B. & Buratowski, S. *Genes Dev.* **13**, 2484–2489 (1999).
18. Grant, P.A. et al. *Cell* **94**, 45–53 (1998).
19. Horikoshi, M., Carey, M.F., Kakidani, H. & Roeder, R.G. *Cell* **54**, 665–669. (1988).
20. Burke, T.W. & Kadonaga, J.T. *Genes Dev* **11**, 3020–3031. (1997).
21. Luger, K. & Richmond, T.J. *Curr. Opin. Struct. Biol.* **8**, 33–40 (1998).
22. Ogrzyzko, V.V. et al. *Cell* **94**, 35–44 (1998).
23. Goodrich, J.A., Hoey, T., Thut, C.J., Admon, A. & Tjian, R. *Cell* **75**, 519–530 (1993).
24. Thut, C.J., Chen, J.L., Klemm, R. & Tjian, R. *Science* **267**, 100–104 (1995).
25. Lu, H. & Levine, A.J. *Proc. Natl. Acad. Sci. USA* **92**, 5154–5158 (1995).
26. Klemm, R.D., Goodrich, J.A., Zhou, S. & Tjian, R. *Proc. Natl. Acad. Sci. USA* **92**, 5788–5792 (1995).
27. Parks, T.D., Leuther, K.K., Howard, E.D., Johnston, S.A. & Dougherty, W.G. *Anal. Biochem.* **216**, 413–417 (1994).
28. Gill, S.C. & von Hippel, P.H. *Anal. Biochem.* **182**, 319–326 (1989).
29. McRorie, D.K. & Voelker, P.J. *Self-associating systems in the analytical ultracentrifuge*. (Beckman Instruments, Inc., Palo Alto; 1993).
30. Cohn, E.J. & Edsall, J.T. *Proteins, amino acids and peptides as ions and dipolar ions* (Reinhold, New York; 1943).